



## Durability and Microstructure Characteristics of Concrete with Supplementary Cementitious Materials

K. J. Brahma Chari <sup>1</sup>, V. Ranga Rao <sup>1\*</sup>

<sup>1</sup> Department of Civil Engineering, Koneru Lakshmaiah Education Foundation, Vaddeswaram, Guntur, Andhra Pradesh, India.

Received 16 November 2021; Revised 12 March 2022; Accepted 23 March 2022; Published 01 April 2022

### Abstract

Considering the environmental impact of cement manufacturing industries, this paper concerns the potential of using supplementary cementitious materials (SCMs), like fly ash and ground granulated blast furnace slag, as being essential to replacing the existing Ordinary Portland Cement (OPC). The objective of this paper is to study the microstructural characteristics of concrete with SCMs and improve the durability of the product to increase the lifespan of concrete structures. Replacement SCMs in OPC are 0, 40, 50, and 60 by percentage of cement weight, and we have taken a water-binder ratio of 0.40 for M40 grade and 0.28 for M60 grade concrete. The physical properties and chemical composition of OPC, Ground Granulated Blast-furnace Slag (GGBS), and fly ash were identified, and three different experiments were conducted to determine the resistance to penetration of chloride ions and corrosion processes. The rapid chloride permeability test, accelerated corrosion, and sorptivity tests were employed to measure concrete's resistance to the effects of aggressive environments and examine the durability properties. The most performed grade samples were analyzed as individual microspheres with Scanning Electron Microscopy (SEM), Energy Dispersive X-Ray Spectroscopy (EDXS), and X-ray diffraction. Significant improvements in various concrete properties were achieved through the partial replacement of fly ash and GGBS with cement.

**Keywords:** Accelerated Corrosion Test; Energy Dispersive X-Ray Spectroscopy; Rapid chloride Permeability Test; Scanning Electron Microscopy; Supplementary Cementitious Materials; X-ray Diffraction Analysis.

### 1. Introduction

The emission of CO<sub>2</sub> into the atmosphere due to the cement manufacturing industry is extremely harmful to humans and the environment. Cement is the second most consumed material after water. Cement is a fundamental and costly constituent of concrete. One hundred and ten kWh of energy and 130 kg of fuel are consumed to manufacture one ton of clinker, the solid intermediary material produced in the manufacture of OPC. This process emits 845 kilograms of CO<sub>2</sub>, with manufactured carbon emissions of 8%. Fly ash and GGBS have been used as additional materials in concrete since the 19<sup>th</sup> and 20<sup>th</sup> centuries [1]. The supplemental cementitious materials utilized in OPC increase the functionality of the solid and decrease the warmth of the hydration of the solid as more breaks appear on the solid surface. The solidity of cement is a vital element in deciding the usefulness of the construction since it influences the mechanical properties, i.e., endurance, synthetic assault, scraping area, and so forth. Chloride particles enter structures and cause decay from multiple points of view, primarily in waterfront territories where sodium chloride can influence solid designs. In this manner, the improvement of the examination work on techniques for the plan of concrete strength [2].

\* Corresponding author: rangarao\_vummaneni@yahoo.com

 <http://dx.doi.org/10.28991/CEJ-2022-08-04-05>



© 2022 by the authors. Licensee C.E.J, Tehran, Iran. This article is an open access article distributed under the terms and conditions of the Creative Commons Attribution (CC-BY) license (<http://creativecommons.org/licenses/by/4.0/>).

In this study combined a proportional mix of different quantities of OPC, fly ash, and GGBS at 60%+20%+20%, respectively, followed by 100%+0%+0%, and (50%+25%+25%). The best performance was achieved by the 60%+20%+20% mix. The curing process for test specimens before applying the test procedure was done at two different timeframes of 28 and 56 days, as previous researchers found pozzolanic activity between the cementitious materials. When compared to ordinary concrete, strength-wise in 28 days, the strength has shown less in proportional mixes, but coming to 56 days, strength-wise, it delivers better results than ordinary concrete. The solid properties of the HVFA supplemented with concrete show the high obstruction in respect of chloride particle penetrability and erosion opposition, and the water interest in substance assault and expansion with the arrangement of C-S-H holding in the solid [3]. Olivia et al. [4] investigated the consumption conduct of steel implanted in fly ash debris GP concrete by a readied sped-up erosion test. The solid examples were presented at a consistent printing voltage of 5 V and 30 V. Two improved fly debris geopolymer concrete blends were contrasted with a control blend (OPC concrete) with a comparable strength grade. Alkalinity decrease by phenolphthalein splash, chloride infiltration by  $\text{AgNO}_3$  shower, and half-cell potential estimation were additionally explored. The speed-up erosion test was done for 28 days.

Golewski (2020) [5] explores the experimental study of the impacts of SCMs in quaternary combinations. Because of the aftereffects of the tests acquired, it was determined that the types of cement made on quaternary fasteners containing nano additives have entirely positive mechanical boundaries. Quaternary types of cement containing 80% OPC, 5% FA, 10% SF, and 5% n's have shown the best outcomes in compressive strength and protection from breakage. Joshi and Pitroda [6] state that the constituents and proportional mixes by appropriate collection and following the excellent construction performance, an almost water-resistant concrete blended mix can be obtained. It is generally advanced based on experimental set-up on test specimens by standard ASTM methods by the time preparing test specimens and curing and testing procedure, which applies current density to steel bars to accelerate the corrosion that affects the bond strength.

Gopalan [7] tested the durability of fly ash concrete compared with cement concrete. Tests were directed to gauge the sorptivity of concrete and fly debris concrete under two diverse restoring conditions. It was reasoned that the impact of relieving on concrete cement was discovered to be considerably less significant. Kubissa et al. [8] restrained sorptivity at 28 days, and 8, 12, 16, 24, 36, 54, and 102 weeks. It was determined that the sorptivity at 28 days is higher compared with the sorptivity at other times. It was additionally demonstrated that the sorptivity at 28 days gives an accurate estimation of the sorptivity of any selection of days. Kim et al. [9] conducted an experimental investigation into fly ash and GGBS setting time, porosity, microstructure, and formation of crystalline phases, and found that they have a lesser effect in developing strength and a denser microstructure. It is evident from XRD patterns that calcium in fly ash did not contribute to forming the C-S-H bond, but the formation of crystalline calcite was observed.

Even though different features of cement-based materials comprise consequential materials, and although nanoparticles have been reported in the literature, the effects of these additives, along with by-products, are poorly documented. It is necessary to study the effect of pulverization based on coal, a by-product of fly ash, and GGBS, a powder additive with a large surface area, on the process ability, pore structure, and durability of RCC. Therefore, in this study, the durability, mechanical, and microstructural properties of mortar containing fly ash and GGBS were investigated. In this regard, the durability characteristics were evaluated using water absorption, electrical resistance, the rapid chloride penetration test (RCPT), the accelerated corrosion test (ACT), and the adsorption test. In addition, the characteristics of the microstructure were evaluated using X-Ray Diffraction (XRD) and Scanning Electron Microscope (SEM) analysis.

## 2. Materials and Methods

In this research, the materials used in the concrete are commercial type Portland cement and mineral admixture. Coal-based pulverized materials like fly ash and GGBS were used. Ordinary Portland Cement-OPC 53 grade cement conforms to IS 12089-1987 [10]. As the researchers stated, the mineral admixture, called supplementary cementitious material, is a coal-based pulverized material called fly ash. According to the manufacturer's report and the test certificates, fly ash can be made to be used on ordinary Portland cement as a supplementary material because clinker emits a high volume of  $\text{CO}_2$  into the environment. The site of the Vijayawada Thermal Power Station (VTPS), Andhra Pradesh (India) [11] was used. It was now coming to the other most workable material, which is GGBS, a by-product of iron factories, JSW-VIZAG. The physical properties such as specific gravity and fineness were tested and found to be 2.6 and 3,600  $\text{cm}^2/\text{gm}$ , respectively. The fine aggregate was free from silt, clay, organic impurities, and clay-free materials mined in the nearby area of Guntur, Andhra Pradesh. The nominal sizes for coarse aggregate are 10 and 20 mm, and they do not contain impurities such as clay particles, organic matter, dust, etc. Preliminary studies ascertained the characterization of these materials.

### 2.1. Properties of Cement and Cementitious Materials (Fly Ash and GGBS)

This study used ordinary grade 53 Portland cement, fly ash, and GGBS. The physicochemical properties of cement, fly ash, and GGBS are shown in Tables 1 and 2.

**Table 1. Physical properties of cement and mineral additives**

Physical properties	Specific gravity	Colour off	Soundness (Le-Chatelier test)	Consistency	Specific surface (Air permeability test)	Bulk density (kg/m <sup>3</sup> )	Initial setting time	Final setting time
Cement	3.14	Grey	1 mm	32.00%	260.45 m <sup>2</sup> /kg	1440	63 minutes	275 minutes
Fly ash	2.53	Greenish	-	34.50%	-	1120-1500	52 minutes	580 minutes
GGBS	2.83	White	-	32.50%	415-460 m <sup>2</sup> /kg	1200	74 minutes	312 minutes

**Table 2. Chemical composition of ordinary Portland cement and mineral admixture as materials**

Composed	SiO <sub>2</sub>	Al <sub>2</sub> O <sub>3</sub>	MnO	P <sub>2</sub> O <sub>5</sub>	MgO	K <sub>2</sub> O	SO <sub>3</sub>	TiO <sub>2</sub>
Blast furnace slag. %	33.57	12.50	-	-	0.98	1.56	-	0.51
Cement clinker. %	22.05	5.15	-	-	1.54	0.74	2.35	-
Fly Ash. %	52.03	21.7	0.01	0.60	0.78	0.69	0.94	1.18

First, the ordinary liquid, the original expendable liquid, which existed unconventionally from an acidic plus accepted matter, remained used for the amalgamation of the concrete. Artificial retort between water and concrete is essential to achieve hardening properties. Second, the applied water should be clean [12]. Superplasticizer is simply discarded to understand its practicality. In addition, fly ash and silica fumes are mainly used as pozzolanic materials in high-strength concrete. These materials are frequently used to enhance the strength of concrete [13].

**Table 3. Mix design details**

Grade name	Water-binder ratio%	Water (kg/m <sup>3</sup> )	Cement (kg/m <sup>3</sup> )	Fly ash (kg/m <sup>3</sup> )	GGBS (kg/m <sup>3</sup> )	Aggregates 20 mm (kg/m <sup>3</sup> )	Aggregates 10 mm (kg/m <sup>3</sup> )	Fine Aggregates (kg/m <sup>3</sup> )	Admixture (kg/m <sup>3</sup> )
M40- 0%	W/B-0.40	157.73	415.07	0	0	691.33	462.58	751.13	2.08
M40- 20%	W/B-0.40	157.73	249.04	83.01	83.01	675.54	452.02	733.98	2.08
M40- 25%	W/B-0.40	157.73	207.54	103.77	103.77	671.60	449.38	729.70	2.08
M40- 30%	W/B-0.40	157.73	166.03	124.52	124.52	667.65	446.74	725.41	2.08
M60- 0%	W/B-0.28	171.20	450.00	208.00	0	604.80	404.70	657.20	4.65
M60- 20%	W/B-0.28	171.20	394.80	131.60	131.60	580.48	388.41	630.70	4.65
M60- 25%	W/B-0.28	171.20	329.00	164.50	164.50	574.00	384.00	623.90	4.65
M60- 30%	W/B-0.28	171.20	263.22	197.42	197.42	567.50	379.73	677.00	4.65

## 2.2. Corrosion Monitoring Techniques

The corrosion monitoring techniques use a combination of cement and mortar to evaluate the erosion behaviour of different steel grades under different conditions. This segment will show the extent of the mortar and solid mixtures and data on the materials used to deliver these blends. Despite the use of a monitoring technique, two specimen tests were conducted on the mixture of mortar and concrete.

## 2.3. ASTM C 1202

Information on experimental design, sample preparation, and testing procedures for corrosion control methods is also provided. From ASTM C 1202, the standard test method that the rapid chloride permeability test is based on, the specimens tested on materials is concrete or a blended mix with composite materials that are called supplementary cementitious materials. Concrete discs are cast, placed over potable water curing under controlled laboratory conditions, and halved for 28 and 56 days, respectively. After each curing time, the sample is removed and stored in a vacuum desiccator for 18 + 2 h. It is placed between two reservoir cells with one cell filled with 3% NaCl solution, while the other is filled with 0.3 molarity of NaOH solution. The two solutions must be mixed in the precise manure with no deviations. Regarding the setup of the RCPT concrete discs, the silicone gel is placed around the concrete discs so no leakages can occur, the power supply machine is supplied at 60 v DC for 6 hrs and a recording is made every 30 minutes. The final reading in coulombs for that one equation is in ASTM C 1202, the standard measurement equation, but the trend has changed in the machine learning so the digital metre is showing the final value of coulombs at 0 hrs, whereas from the above procedure, the penetration of chloride ions can be measured by a standard table that provides data with extreme conditions to deficient requirements [14].

**2.4. Accelerated Corrosion Test**

This is the rapid test method where the chloride ion penetrates through the 3% concentration NaCl solution and also a steel bar which is embedded in concrete by taking a non-corrosive steel bar, which will be kept inside the concrete. A 40 mm cover was taken from one phase of the test sample and the bottom of the same cover had 15 V DC supplied to the steel bar continuously without taking any breaks. If a test specimen was corroded then that particular specimen was removed from the setup and the remaining specimens continued to process until the last bar was corroded by deflection of the passive layer which protects the reinforcement against corrosion [15]. Figure 1 shows the variation of penetrations of chloride ions in the form of liquid that is a 3% concentration of NaCl solution.

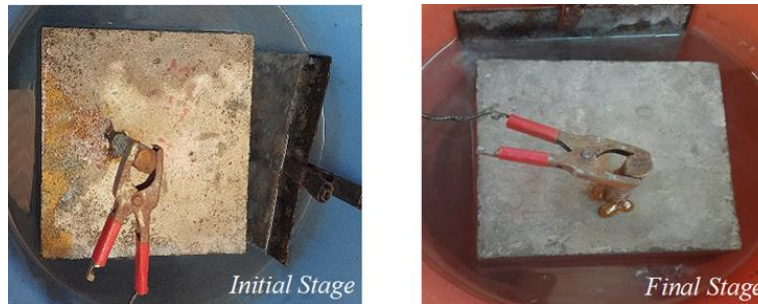


**Figure 1. Initial stages and final stages of accelerated corrosion test setup of M40 W/B-0.40**

This accelerated corrosion test was applied to two grades with different W/B ratios and different proportional mixes. M40 and M60 grades were used with balanced mixtures of four different types, i.e., common mix, proportional mix 1, balanced mix two, and balanced mix 3. These had cement-based material replacement with different ratios of fly ash and GGBS. The test specimens were cube-shaped of 150mm x 150mm in size and were placed into deep saline water of 5% concentration until the required results were obtained. The accelerated setup rebar was kept in the concrete specimen with 40 mm cover formed into two phases, from the bottom and side cover. As the chloride ions penetrated the specimen the solidity of the cubes would slowly fail, showing initial cracks and total damage. As per the test, the obtained results show some differences in the grade variation and within proportions to different replacements in cementitious materials. The M60 grade concrete showed higher resistance to the absorption of chloride ions into the concrete specimen (Figure 2).

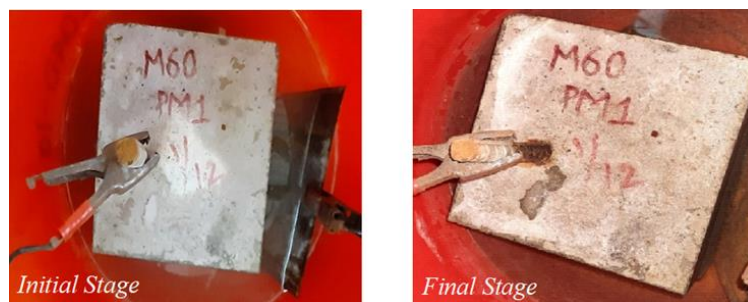


**Figure 2. Accelerated corrosion test setup of M60 W/B-0.28 Initial to Final stages**

**2.5. Sorptivity**

The Sorptivity can be monitored by estimating the rate at which the capillary increase is maintained in a substantially homogenous material. After the design, the chamber was flooded with water for 90 days. After drying in a broiler at 100+10°C, a sample measuring 100 (width) × 50 (height) mm was suffocated at a water level not exceeding 5 mm above the base sample, and the fringe surface stream was forestalled by appropriately fixing with a non-spongy liner. The amount of water consumed in a short time was estimated by measuring this example on a scale with an upper pan weighing up to 0.1 mg. The water on the outside of the sample was cleaned with a damp cloth, and each weighing operation was completed in 30 seconds. The uptake of collected water (per unit area of the surface) increased with time (t) of the square foundation [16].

$$I = S \cdot t^{\frac{1}{2}} \tag{1}$$

$$S = \frac{I}{t^{\frac{1}{2}}} = \frac{\left(\frac{\Delta w}{AD}\right)}{t^{\frac{1}{2}}}; \left(\frac{\Delta w}{AD}\right) = \frac{\text{Weight of cylinder after 30 minutes (W2)} - \text{Oven dry weight of cylinder in grams (W1)}}{\text{Sample surface area where water has entered (A) X Density of water (D)}} \tag{2}$$

where S is Sorptivity in mm, t is elapsed time in minutes.

### 3. Results and Discussion

#### 3.1. Rapid Chloride Permeability Test

The rapid chloride permeability test (RCPT) is the standard technique to measure the durability of concrete, particularly penetration by chloride ions by the electrical insulation on the reservoir cells by a standard solution of 3% concentration of NaCl, and 0.3 M of NaOH solutions in 60 v DC is supplied through an electrically conductive wire into the NaCl solution for 6 hrs. Now coming to the values in the coulombs to the mix proportions supplemented in OPC with varies with 0, 20, 25, and 30%. The same procedure is used for 28 and 56 days, respectively. As shown in Figures 3 and 4, the ranges of chloride ion penetration into concrete discs shown by the by RCPT, as the graphs show that in the Water-Binder (W/B) ratio of 0.40 with different ratios in replacement of mineral admixture in OPC. The mix with 0% replacement shows the high range of chloride ion penetration in twenty-eight days were coming to the fifty-six days in the same proportions states that moderate range of chloride ions into specimens and compare with the 30% replacement at the age of 28 days also chloride ions penetration is low. At 56 days, the chloride ions flow of penetration into concrete is deficient, which means it is very effective with high replacement of cementitious materials in OPC. The replacement of 20 and 25% are at moderate and low ranges of penetrations of chloride ions in specimens, the penetration of 25% replacement of composite cementitious materials also shown effective results and tested on multiple grades [14].

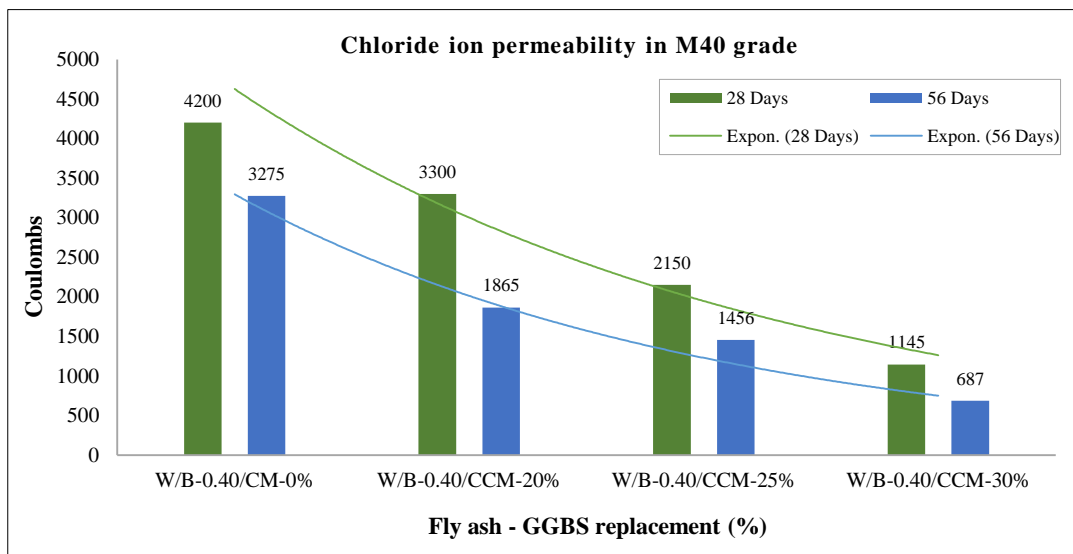


Figure 3. Coulombs vs. (%) Replacement of Fly Ash and GGBS

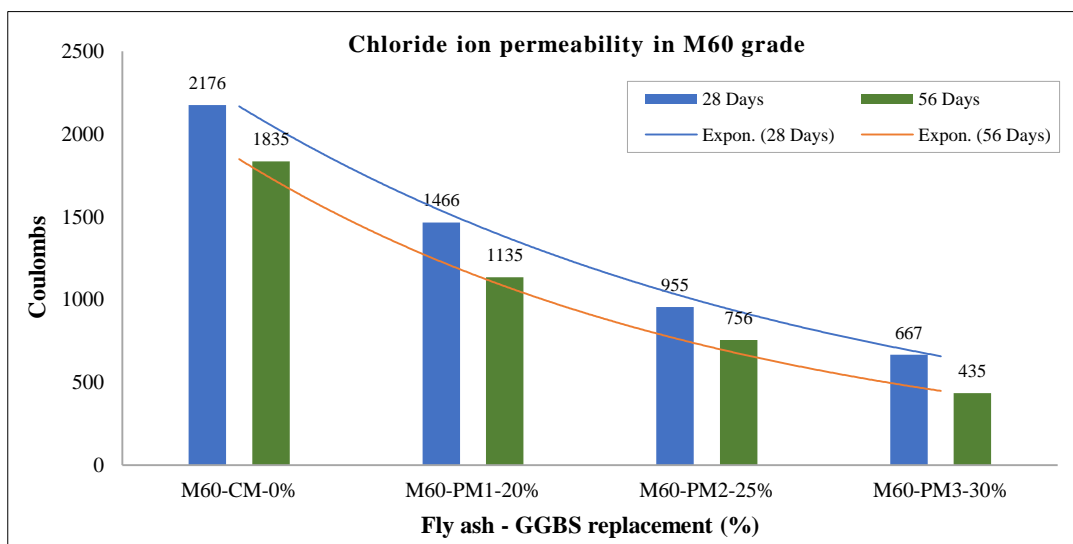


Figure 4. Coulombs vs. (%) Replacement of Fly Ash and GGBS

#### 3.2. Accelerated Corrosion Test

Table 4 shows the corrosion initiation of the rebar and cracking time. Table 4 shows the corrosion initiation of rebar data on corrosion initiation time and cracking time (days). The electric flow perusing is taken from a simply advanced meter. To quantify the consumption rate, we played out a speeded-up corrosion test by applying 15 V DC to the rebar installed in the solid covering, that is a 40 mm cover. This tests various extents of cement with substitutions of fly debris and GGBS in the mix. The rates that are changed in OPC are 0, 20, 25, and 30%.

**Table 4. Corrosion initiation of rebar and cracking time**

Sample ID	Corrosion initiation time (days)	Cracking time (days)
M40-CM-0%	4	6
M40-PM1-20%	7	10
M40-PM2-25%	11	17
M40-PM3-30%	15	22
M60-CM-0%	7	10
M60-PM1-20%	13	16
M60-PM2-25%	17	23
M60-PM3-30%	22	32

**3.3. Sorptivity**

The sorptivity is the ability of the test sample to absorb or desorb liquid in a specific time frame. In this research, the test was conducted on supplementary cementitious materials with different replacement ranges in OPC. The water absorption test was carried out in laboratory conditions under a controlled examination method. Before that, the test specimens of concrete discs were kept in the oven to dry for three days at 50°C then removed from the oven and kept in a laboratory for 24 hours, to come to room temperature. The samples were panelled now, and the results obtained from a standard procedure is shown in Figure 5, that the control mix (CM) is 2.6, this value representing the absorption in mm in the concrete test sample, and the composite cementitious materials (CCM) with various percentages are 20%, 25%, and 30%. The CCM proportions are statistically decreasing the sorptivity in mm which indicates that water absorption is less when compared with the common mix. The sorptivity of 30% replacement is 1.8 which is less water demand at 2.3 and 2.1, respectively.

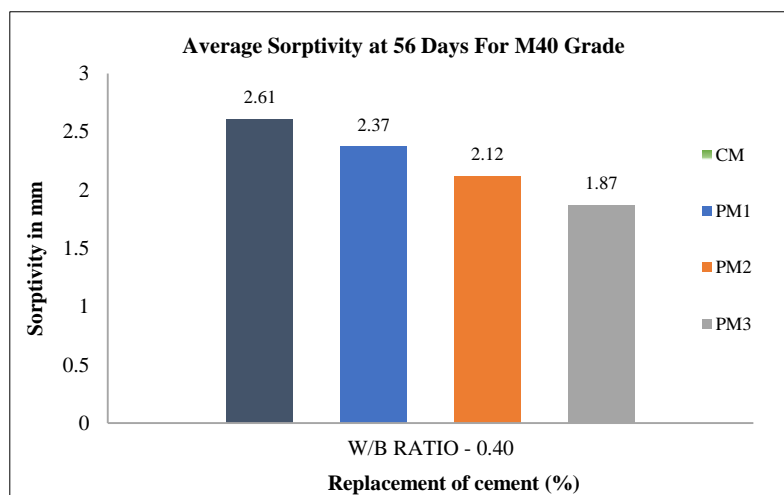


**Figure 5. Sorptivity vs. Replacement of Cement (%)**

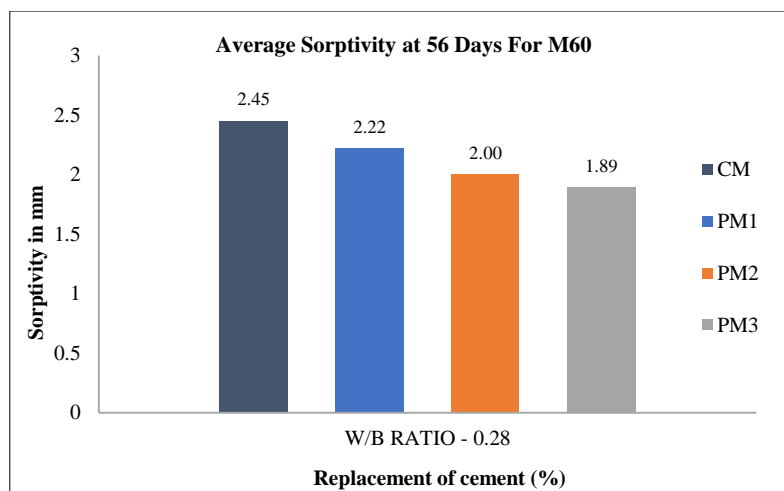


**Figure 6. Sorptivity vs. (%) Replacement of Cement**

### 3.4. SEM Analysis

At first, the concrete specimens are broken into small fragments. We can see from the SEM micrograph shown below in Figure 7, the rapid spread of the C-H-S gel on the hydrated cement paste is the leading cause of strength. The standard mix, which shows less hydrated practices than 50% of fly ash and GGBS in the ratio of 25% each, shows more C-H-S gel with the increase in hydration on the cement paste in Figure 9 where we see calcium and silicon due to the dissolution reaction of the GGBS to form C-S-H. As shown in Figures 8 and 10, the Energy-dispersive X-ray spectroscopy (EDX) analysis graphs are peaks defining the elements O, Si, and Ca are higher than the other elements in the blended mix with respect to both mix proportions used in the analysis. The SEM images show there are more voids in the control mix than the proportion mix. Finally, the results are more effective in the proportional combinations [17, 18].

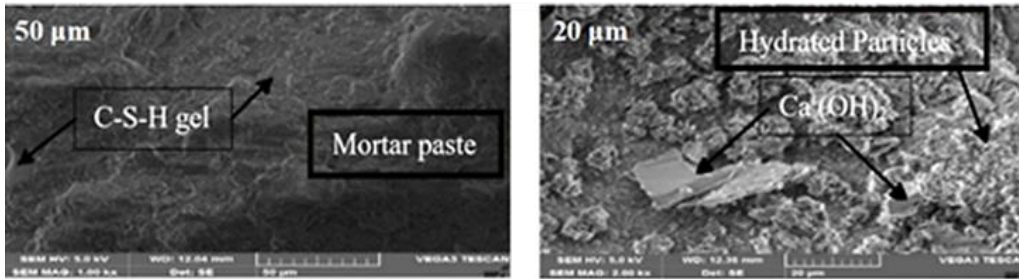


Figure 7. SEM images of M40 grade - W/B – 0.40 mix (100% C)

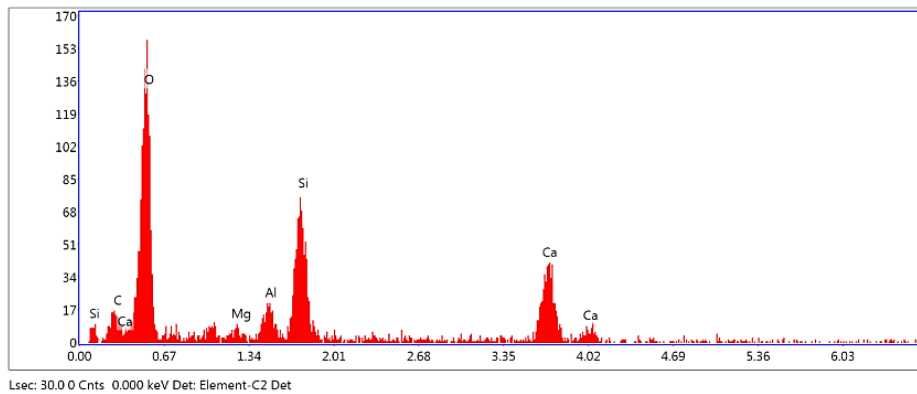


Figure 8. EDX Analysis of M40 grade - W/B – 0.40 mix (100% C)

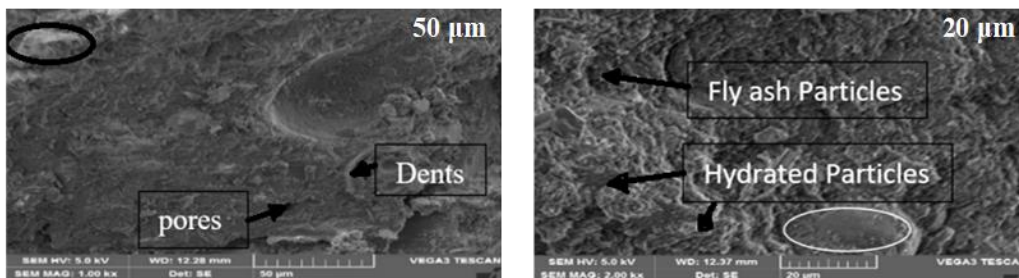


Figure 9. SEM images of M40 grade - W/B – 0.40 mix (50% C + 25% F. A + 25% G.G.B.S)

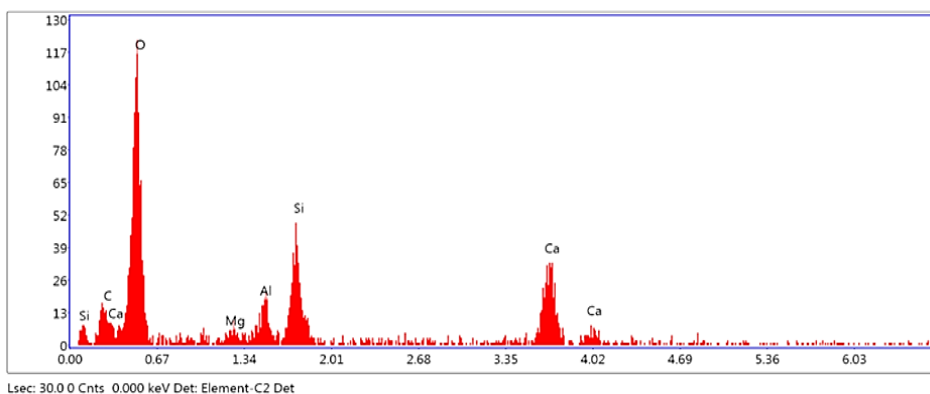


Figure 10. EDX Analysis of M40 grade - W/B – 0.40 mic (50% C+25% F. A + 25% G.G.B.S)

The SEM micrograph shown in Figure 11 shows the rapid spread of C-H-S gel on the hydrated cement paste, which was the leading cause of strength. The standard mix, which shows less hydrated practices than 50 % of F.A and G.G.B.S in the ratio of 25%, each shows more C-H-S gel with the increase in hydration on the cement paste as shown in Figure 13, calcium and silicon due to the dissolution of GGBS react to form C-S-H. As shown in Figures 12 and 14, elements such as Si, Ca, Mg and Al present in the EDX spectrum are due to the mixed compositions of GGBS and cement and C and O elements due to fly ash. The fluctuations of peaks in the spectrum are due to varied cement, GGBS, and fly ash compositions.

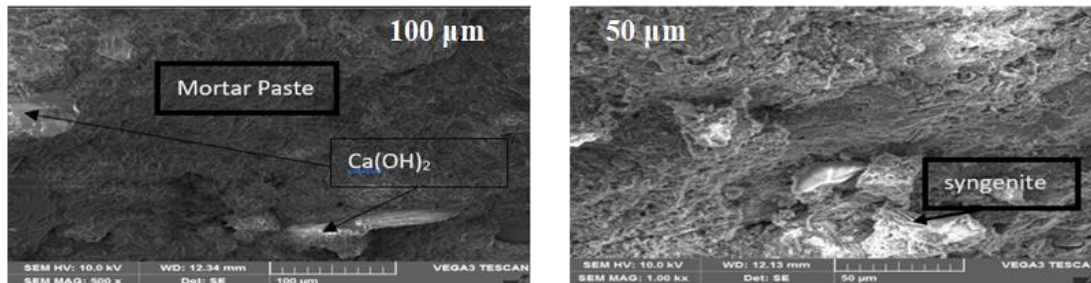


Figure 11. SEM Micrograph W/B - 0.28 of Mix (60% C + 20% F. A + 20% G.B.B.S)

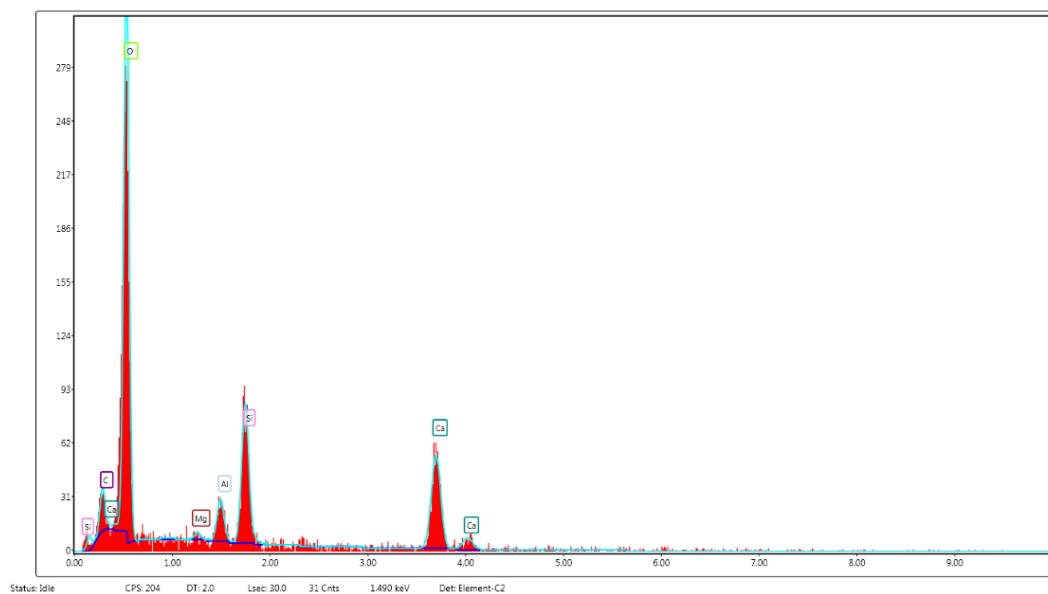


Figure 12. EDX Analysis W/B - 0.28 of Mix (60% C+20% F.A + 20% G.B.B.S)

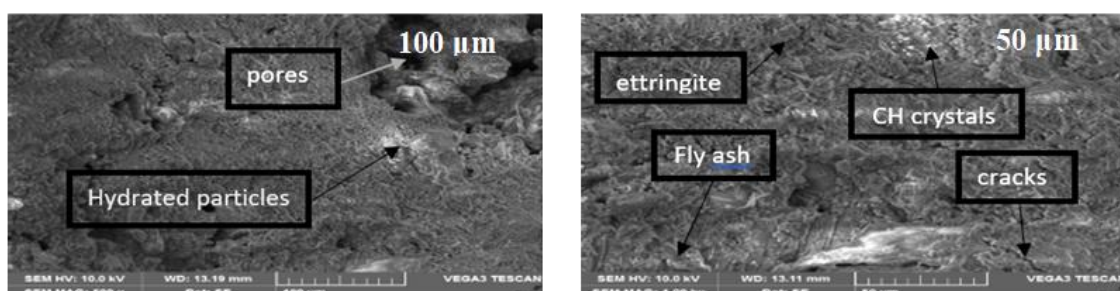


Figure 13. SEM Micrograph W/B - 0.28 of Mix (50% C + 25% F. A + 25% G.B.B.S)

### 3.5. XRD Analysis

The soil phase and component fly ash and GGBS were performed using an XR diffractometer, a Shimadzu XRD-6000. The sample was made in powder form. XRD analysis was performed using CuK radiation using X-ray tubes operating at 40 kV and 35 mA. XRD data were collected in two values ranging from 10° to 80°, with a scan rate of 2° per minute and a scan step of 0.02°. Match software High Score Plus was used for an automatic search to analyse diffraction data.



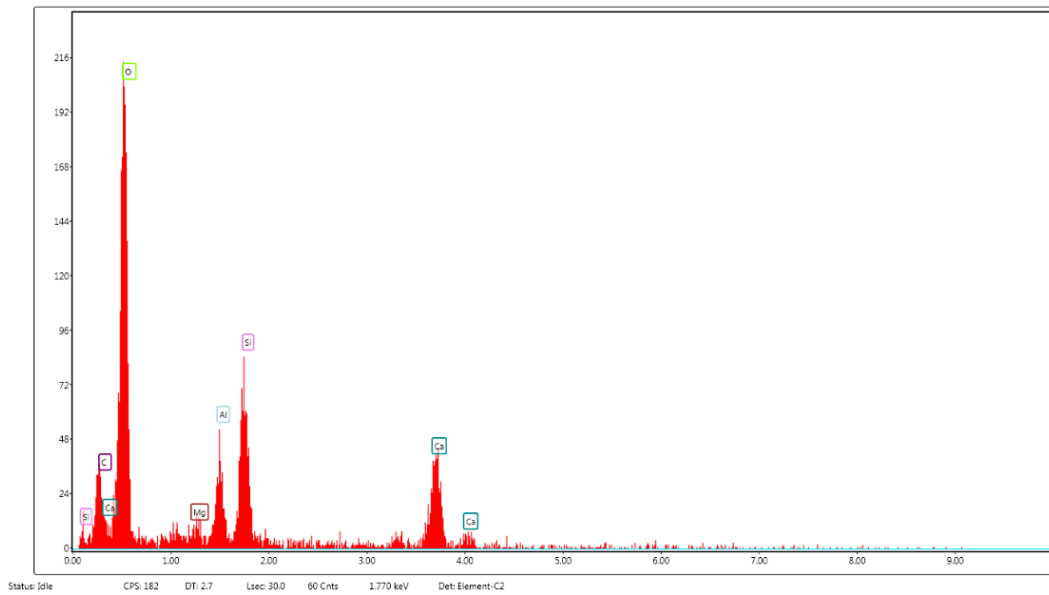


Figure 14. EDX Analysis W/B - 0.28 of Mix (50% C + 25% F. A + 25% G.B.S)

Figures 15 show the XRD results of cement pastes with varying amounts of fly ash and GGBS. As shown in the XRD diagram, the mullite and quartz tops of the first fly debris remained after the antacid system was activated and the GGBS expanded. An example of diffraction with 0% GGBS shows a hazy mound at 15° to 40° (2θ), confirming the arrangement of the gel without mixed morphology. The ambiguous properties of the geopolymer did not change when GGBS was presented in the blend. In each case, a new diffraction peak was found to occur near the 30° (2θ). This was thought to be the generation of hydrated calcium silicate. The expansion of GGBS in the blend increases the most important strength of C-S-H indicating an increase in the placement of hydrated calcium silicate [19]. For sustainable concrete development, 100% substitute for RCA and 30% substitute for fly ash cement were used. The inclusion of silica fume and steel fibres significantly improved the performance of recycled aggregate concrete at elevated temperatures. The optimal dose of glass fibre was determined to be 0.25% in the experiment (Table 3) [20-22]. The durability was determined according to the method proposed by Koch and Steinegger, and the optimum SCM replacement ratio was 30%, which increased efficiency and compressive strength [23-25].

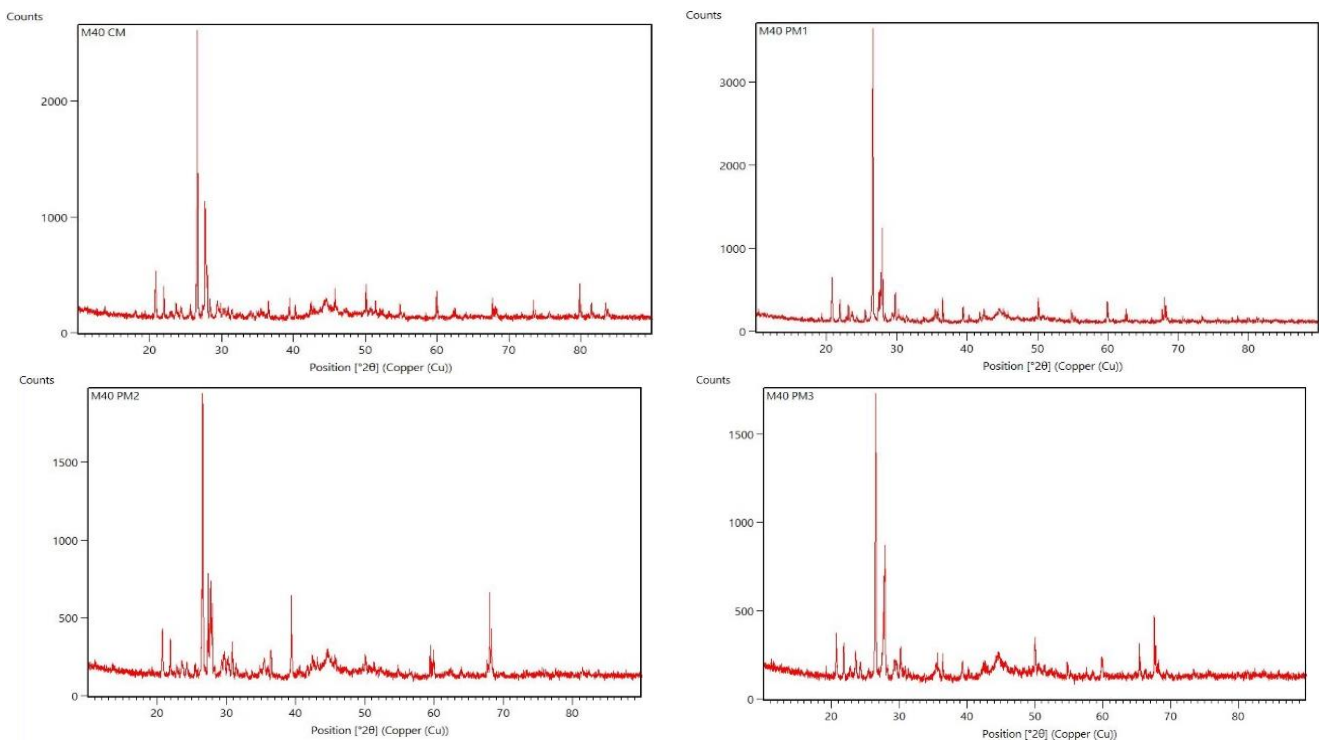


Figure 15. XRD Analysis of M40 grade for replacement of F.A & G.G.B.S with different proportions

As per the JCPDS data, the phases present in Figure 16 as follows:

The peaks appearing at 28°, 36°, 46°, and 50° are due to calcium hydroxide ( $\text{Ca}(\text{OH})_2$ ); 36°, 55°, 81°, and 84° are due to calcium oxide ( $\text{CaO}$ ); 27°, 31° and 40° are due to tricalcium silicates (alite) ( $\text{C}_3\text{S}$ ); 46°, 60° and 80° dicalcium silicates (belite) ( $\text{C}_2\text{S}$ ); 22° and 29° are due to calcium carbonate ( $\text{CaCO}_3$ ); 45° and 68° are due to magnesium oxide ( $\text{MgO}$ ); 21° and 24° are due to calcium sulphate ( $\text{CaSO}_4$ ); 39°, 50° and 63° are due to calcium silicate ( $\text{Ca}_2\text{SiO}_4$ ) 46°, 52°, 60°, and 80° are due to tricalcium aluminate ( $\text{Ca}_3\text{Al}_2\text{O}_6$ ).

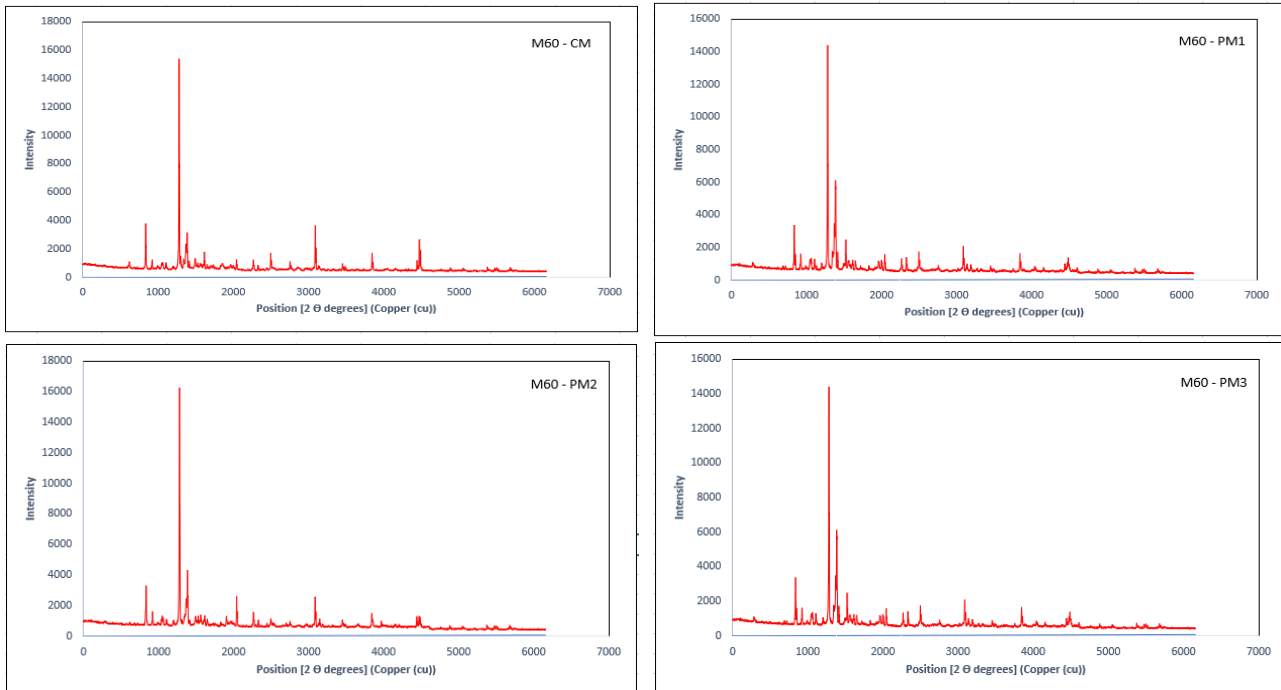


Figure 16. XRD Analysis of M60 grade for replacement of F.A and G.B.S with different proportions

## 4. Conclusion

In this study, the microstructure and durability of concrete were investigated by adding supplementary cementitious materials such as fly ash and GGBS obtained from industrial by-products. The concrete cubes were tested for accelerated corrosion by the rapid initiation of the corrosion process for 56 days. In the case of cement replacement with supplementary cementitious materials, there were improved results. When 30% of fly ash and 30% of GGBS are substituted with cement, it takes a longer time to initiate corrosion and cracking and an increased damage period of the specimen in M40 and M60 grades. When 20% of fly ash and 20% of GGBS were substituted with cement, a high compressive strength resulted, but it was observed that a low range of deficient coulombs values was obtained during the durability test of the rapid chloride penetration process compared to 60% SCMs specimens. The specimens containing 60% SCMs have a lower sorption capacity in mm compared with the 40% SCM specimens.

SEM analysis shows that the inclusion of fly ash and GGBS in the mixture produces an additional calcium silicate hydrate gel, which helps to achieve reasonable durability with 60% SCM specimens in the M40 and M60 grades. The hydration rate of 40% SCM specimens was like that of a normal concrete mixture, but the presence of mineral elements was significantly different from that of the control mix, which altered the strength of the concrete mixture. The faster formation of hydration products in the presence of fly ash and GGBS nanoparticles is confirmed by the XRD results and is the reason for the improved durability.

## 5. Declarations

### 5.1. Author Contributions

Conceptualization, J.B.C.K. and R.R.V.; methodology, J.B.C.K.; validation, R.R.V.; formal analysis, J.B.C.K.; investigation, J.B.C.K.; data curation, J.B.C.K.; writing—original draft preparation, J.B.C.K.; writing—review and editing, R.R.V.; supervision, R.R.V.; funding acquisition, R.R.V. All authors have read and agreed to the published version of the manuscript.

### 5.2. Data Availability Statement

The data presented in this study are available on request from the corresponding author.

### 5.3. Funding

The authors received no financial support for the research, authorship, and/or publication of this article.

### 5.4. Acknowledgements

The authors would like to thank the Department of Civil Engineering and the Koneru Lakshmaiah Education Foundation for supporting the experimental work. The authors are grateful to acknowledge the Department of Science and Technology (DST), Govt. of India, for the award of the DST-FIST Level-1 (SR/FST/PS-1/2018/35) scheme to the Department of Physics, KLEF for supporting the XRD analysis. Also thank the Department of science and technology (DST), to Vignan's Foundation for Science, Technology and Research for supporting the experimental work on SEM and EDX analysis.

### 5.5. Conflicts of Interest

The authors declare no conflict of interest.

## 6. References

- [1] Giergiczy, Z. (2019). Fly ash and slag. *Cement and Concrete Research*, 124, 105826. doi:10.1016/j.cemconres.2019.105826.
- [2] Gade, P., Chari Kanneganti, J. B., & Vummaneni, R. R. (2020). Durability study on multiple grades of concrete with ternary blend supplementary cementitious materials. *Materials Today: Proceedings*, 33, 925–933. doi:10.1016/j.matpr.2020.06.452.
- [3] Pal, S. ., Mukherjee, A., & Pathak, S. (2003). Investigation of hydraulic activity of ground granulated blast furnace slag in concrete. *Cement and Concrete Research*, 33(9), 1481–1486. doi:10.1016/s0008-8846(03)00062-0.
- [4] Olivia, M., & Nikraz, H. R. (2011). Corrosion performance of embedded steel in fly ash geopolymer concrete by impressed voltage method. *Incorporating Sustainable Practice in Mechanics of Structures and Materials - Proceedings of the 21st Australian Conference on the Mechanics of Structures and Materials*, 781–786. doi:10.1201/b10571-141.
- [5] Golewski, G. L. (2020). Energy Savings Associated with the Use of Fly Ash and Nan additives in the Cement Composition. *Energies*, 13(9), 2184. doi:10.3390/en13092184.
- [6] Joshi, G., & Pitroda, J. R. (2018). Evaluation of Sorptivity and Water Captivation of Concrete with Partial Replacement of Cement by Hypo Sludge. *IOP Conference Series: Materials Science and Engineering*, 431, 032010. doi:10.1088/1757-899x/431/3/032010.
- [7] Gopalan, M. K. (1996). Sorptivity of fly ash concretes. *Cement and Concrete Research*, 26(8), 1189–1197. doi:10.1016/0008-8846(96)00105-6.
- [8] Kubissa, W., & Jaskulski, R. (2013). Measuring and time variability of the sorptivity of concrete. *Procedia Engineering*, 57(June), 634–641. doi:10.1016/j.proeng.2013.04.080.
- [9] Sasui, S., Kim, G., Nam, J., Koyama, T., & Chansomsak, S. (2020). Strength and microstructure of class-C fly ash and GGBS blend geopolymer activated in NaOH & NaOH + Na<sub>2</sub>SiO<sub>3</sub>. *Materials*, 13(1). doi:10.3390/ma13010059.
- [10] Bureau of Indian Standards (BIS), IS-12089. (1987). Specification for granulated slag for the manufacture of Portland slag cement, New Delhi, India.
- [11] Bureau of Indian Standards (BIS), IS-3812-1. (2013). Specification for Pulverized Fuel Ash, Part 1: For Use as Pozzolana in Cement, Cement Mortar and Concrete. Bur. Indian Stand. New Delhi, India.
- [12] Bureau of Indian Standards (BIS), IS-56. (2000). Concrete, Plain and Reinforced. Bur. Indian Stand. New Delhi, India.
- [13] Bureau of Indian Standards (BIS), IS-9103. (1999). Specification for Concrete Admixtures BIS. New Delhi, India.
- [14] ASTM C-1202. (2012). Standard Test Method for Electrical Indication of Concrete's Ability to Resist Chloride Ion Penetration. American Society for Testing and Materials, 1–8. doi:10.1520/C1202-12.2.
- [15] Abouhussien, A. A., & Hassan, A. A. A. (2014). Experimental and Empirical Time to Corrosion of Reinforced Concrete Structures under Different Curing Conditions. *Advances in Civil Engineering*, 2014, 1–9. doi:10.1155/2014/595743.
- [16] Afroz, S., Rahman, F., Iffat, S., & Manzur, T. (2015). Sorptivity and Strength Characteristics of Commonly Used Concrete Mixes of Bangladesh. In *International Conference on Recent Innovation in Civil Engineering for Sustainable Development*, 39–44.
- [17] Trejo, D., Halmen, C., & Reinschmidt, K. (2009). Corrosion performance tests for reinforcing steel in concrete: Technical Report (No. FHWA/TX-09/0-4825-1). Texas Transportation Institute, Texas, United States.
- [18] Saludung, A., Ogawa, Y., & Kawai, K. (2018). Microstructure and mechanical properties of FA/GGBS-based geopolymer. In *MATEC Web of Conferences* (Vol. 195, p. 01013). EDP Sciences. <https://doi.org/10.1051/mateconf/201819501013>.

- [19] Rizki Abdila, S., Mustafa Al Bakri Abdullah, M., Faheem Mohd Tahir, M., Ahmad, R., Syafwandi, & Isradi, M. (2020). Characterization of Fly ash and Ground Granulated Blast Slag for Soil Stabilization Application Using Geopolymerization Method. *IOP Conference Series: Materials Science and Engineering*, 864(1). doi:10.1088/1757-899X/864/1/012013.
- [20] Hasan, Z. A., Abdulridha, S. Q., & Abeer, S. Z. (2021). Sustainable Mortar Made with Local Clay Bricks and Glass Waste Exposed to Elevated Temperatures. *Civil Engineering Journal*, 7(8), 1341–1354. doi:10.28991/cej-2021-03091729.
- [21] Das, M., & Mishra, S. P. (2020). Parametric Strategy for Composite Cement Concrete Blended with Fly Ash & Glass Fiber. *Current Journal of Applied Science and Technology*, 162–176. doi:10.9734/cjast/2020/v39i3531065.
- [22] Raza, A., Ali, B., Haq, F. U., Awais, M., & Jameel, M. S. (2021). Influence of fly ash, glass fibers and wastewater on production of recycled aggregate concrete. *Materiales de Construccion*, 71(343), 253. doi:10.3989/MC.2021.15120.
- [23] Memon, M. A., Memon, N. A., & Memon, B. A. (2020). Effect of Fly Ash and Un-crushed Coarse Aggregates on Characteristics of SCC. *Civil Engineering Journal*, 6(4), 693–701. doi:10.28991/cej-2020-03091501.
- [24] Gade, P., Chari Kanneganti, J. B., & Vummaneni, R. R. (2020). Durability study on multiple grades of concrete with ternary blend supplementary cementitious materials. *Materials Today: Proceedings*, 33, 925–933. doi:10.1016/j.matpr.2020.06.452.
- [25] Sáez Del Bosque, I. F., Sánchez de Rojas, M. I., Medina, G., Barcala, S., & Medina, C. (2021). Durability of ternary cements based on new supplementary cementitious materials from industrial waste. *Applied Sciences (Switzerland)*, 11(13), 5977. doi:10.3390/app11135977.